1970

The strength of heavy welded box columns, December 1970 (Beer's M.S.)

Gernot Beer

Lambert Tall

LEHIGH UNIVERSITY

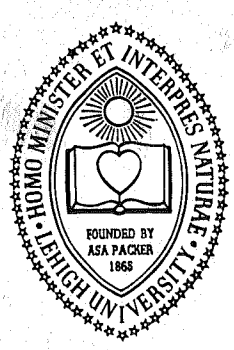

OFFICE OF RESEARCH

Residual Stresses in Thick Welded Plates

THE STRENGTH OF HEAVY WELDED BOX COLUMNS

by

Gernot Beer

Lambert Tall

Fritz Engineering Laboratory
Department of Civil Engineering
Lehigh University
Bethlehem, Pennsylvania

December, 1970

Fritz Engineering Laboratory Report No. 337.27

TABLE OF CONTENTS

ABSTRACT

This report presents the results of an investigation on a heavy welded box shape 24" x 24" x 2", designated 24 □ 774. The study was both experimental and theoretical.

The experiments reported are residual stress measurements and tension coupon tests. The influence of the manufacturing procedure on the formation of residual stress was investigated.

The theoretical part deals with the prediction of the maximum strength of box columns. A computer program was developed to compute maximum strength curves. The influence of some of the main factors such as residual stress, initial out-of-straightness and size of the shape, on the maximum strength is shown.

It is concluded that the welding procedure has the most significant influence on the formation of residual

stress, especially the welding sequence, since it will cause the residual stress distribution to be unsymmetrical, and that the unsymmetric residual stress can have some influence on the maximum strength. From comparison of the heavy box shape investigated with respect to a considerably lighter shape (10□61) it has been found that the heavy shape has a smaller magnitude of compressive residual stress, and that slender heavy columns ($L/r > 80$) can be as much as 20% stronger than slender light columns if compared on a non-dimensionalized basis.

ACKNOWLEDGEMENTS

This report presents a part of an investigation carried out in the overall research project, "Residual Stresses in Thick Welded Plates". The research program is being conducted at Fritz Engineering Laboratory, Department of Civil Engineering, Lehigh University, Bethlehem, Pennsylvania. Dr. Lynn S. Beedle is the Director of Fritz Engineering Laboratory, and Dr. D. A. VanHorn is the Chairman of the Department of Civil Engineering.

The investigation is being carried out under the sponsorship of the National Science Foundation, and the Column Research Council. The technical guidance of Task Group 1 of the Column Research Council under the chairmanship of John A. Gilligan is sincerely appreciated.

The test specimen was manufactured by the Bethlehem Steel Corporation. Sincere appreciation is expressed to this company and to its personnel.

The authors are indebted to Jacques Brozzetti who commenced this portion of the study and to Reidar Bjørhovde and Negussie Tebedge for their assistance at all times.

Thanks are due to Kenneth Harpel, Laboratory Superintendent, and his staff for the excellent preparation of the test specimens.

Special thanks are due to Richard Sopko for the photography, to John Gera for preparing the drawings, and to Miss Joanne Mies for typing the entire manuscript.

1. INTRODUCTION

Heavy shapes are being used increasingly in large structures. The applications include the lower stories of multi-story buildings, large bridges, assembly buildings for space vehicles, and many more.

Some heavy column shapes used in existing structures are shown in Fig. 1. In this paper, heavy shapes are defined as sections with component plates exceeding 1 inch in thickness. Very little information is available about the strength of such members, since previous investigations dealt only with small and medium size shapes.

Almost 20 years ago it was shown[1,2] that residual stresses have a significant influence on the strength of members subjected primarily to axial compression.

An extensive research program is being carried out at Lehigh University to study residual stresses in

heavy shapes made of A36 steel. Figure 2 shows the shapes being investigated; the first five shapes have already been measured.[3]

The study presented here describes the investigation of a heavy box-shape, 24□774. The residual stress distribution is presented and related to the manufacturing procedure, and the results are compared with residual stresses in a medium-size shape.

A computer program was developed based on a theoretical approach described in Ref. 4 to study the influence of main factors such as residual stress, initial out-of-straightness and size of the shape, on the maximum strength of a column.

2. MANUFACTURING PROCEDURE

The manufacturing and fabrication conditions can have a major influence upon the magnitude and distribution of residual stress and yield stress. Therefore the actual conditions during manufacture of the box-shape were recorded.

The recording includes information about chemical and mechanical properties of the heat, rolling, flamecutting and welding procedure. These data were recorded together with that for a number of medium-size to heavy test specimens, which were ordered for residual stress measurements in two research projects, "Welded Columns and Flame-Cut Plates" and "Residual Stresses in Thick Welded Plates".[5]

2.1 Rolling of the Parent Plates

The rolling process consists of two phases: the initial rolling and the final rolling. Figure 3 shows a schematic diagram of the rolling process.

First the ingot is heated to 2400°F in a furnace. Then the ingot is passed through a first rolling stand, which gives the plate the approximate required dimension. Figure 4 shows this phase of the rolling. The final rolling stand brings the plate to the required dimensions. Table 1 shows the chemical and mechanical properties of the heat as given in the mill test report.

After rolling the plates are placed on the cooling bed. Temperature measurements were made at the cooling bed using "Templestik" temperature crayons, provided in increments of 50°F. The variation of temperature across the plates was not measured. The result of the temperature measurements are plotted in Fig. 5.

2.2 Flame Cutting

The parent plates were rolled to sizes 2" wider than that required. One inch strips were cut later from each edge; a standard burning machine with two torches was used to burn both edges simultaneously. The travel

speed was set to about 10 inches per minute. For transverse cutting the same speed and only one torch was used. Temperature measurements were made by drawing lines on the plate surface using the "Templestick" crayons. The location of measurements relative to the torches is shown in Fig. 6. The temperature distribution due to flame-cutting is shown in Fig. 7.

2.3 Welding

The 7/8" groove welds were deposited by a semi-automatic welding machine, the Lincoln ML $2\frac{1}{2}$. A 5/32" diameter electrode wire was used which conformed to the AWS class E7018. Shielding was accomplished by a granular flux, 780 type.

Figure 8 shows the welding in process. Fit was made by tack and seal welds arc-welded with E7018 electrodes of 5/32" diameter. Figure 9 shows a seal weld being placed. Preheating was manual and according to the AWS specifications.[6] A maximum of 11 and a minimum of 9 passes was used for each weld. The approximate size of

one pass can be seen in Fig. 10. The welding conditions were such that the voltage was 33 Volts and the amperage was 400 Amperes, the welding speed varied from 26 to 14 inch per minute.

3. RESIDUAL STRESS MEASUREMENTS

3.1 Sequence of Sectioning

For the measurement of the residual stress distribution across the shape, the method of sectioning as described in detail in Ref. 7 was used. This method allows the measurement of the longitudinal residual stresses in a specimen by cutting it into a large number of sections. The distance between two points is measured before and after the sectioning procedure; the relieved strain can be computed, and is equal to the residual strain assuming that all the residual stress has been relieved by the sectioning. The residual stress can then be obtained by multiplying the strain with the Young's Modulus, assuming a completely elastic behavior.

First gage holes were laid out on the specimen and the initial readings were taken. Then the 7'-3" long specimen was reduced to the 14" long residual stress specimen with two transverse cuts. A circular cold-saw with a diameter of about 6' and a thickness of 1" was used. Figure 11 shows the transverse cutting. Then two

longitudinal cuts were used to separate the top and bottom plates from the side-plates using the same cold-saw. Originally it was planned to section the component plates. Final readings should be taken after this procedure.

During the longitudinal cutting the inside of the side-plates were scraped and several gage-holes were destroyed, by accident. Figure 12 shows a photo of the destroyed surfaces. The original plan was then changed to save as many results as possible.

Measurements were taken on the gage holes which were not destroyed. Thus the stress-relief after partial sectioning, that is, after separating the component plates, could be computed at these locations. New gage points were drilled on the inside surfaces of the side plates, and new initial readings were taken. Then the plates were sectioned as planned. Measurements were taken again and the additional stress relief due to final sectioning was computed. The final residual stress distribution was then computed by adding the residual stress obtained after

partial sectioning to the residual stress obtained from sectioning the component plates.

As pointed out, some gage holes were destroyed at the inside surfaces and a residual stress distribution after partial sectioning had to be assumed for these locations. Figure 13 shows the distribution which was assumed. This assumption was obtained by using the distribution at the lower part of the right side-plate, Figure 14.

3.2 Results

The reduction of data was made using a digital computer. The procedure and the relevant computer programs are described in detail elsewhere.[8] Automatic plots of the distribution of residual stress in the component plates were obtained using a digital plotter. This distribution after partial and final sectioning can be seen in Figs. 15 and 16. The final result is plotted in Fig. 17. The equilibrium conditions:

$$P_{int} = \Sigma \sigma_r = 0 \qquad (1a)$$

$$M_{x,int} = \Sigma \sigma_r y = 0 \qquad (1b)$$

$$M_{y,int} = \Sigma \sigma_r x = 0 \qquad (1c)$$

were checked.

The average out-of-equilibrium stress was -1.4 ksi. This is mainly due to the fact that residual stresses had to be assumed for the destroyed regions of the side-plates. However, compared with out-of-equilibrium stresses obtained from measurements on other shapes,[3] which vary between $\pm$0.6 and $\pm$1.0 ksi, the error is not very large. The distribution was adjusted for equilibrium by applying the computed out-of-equilibrium force and moments in the opposite direction and adding the resulting stresses to the residual stresses. Figure 18 shows the final average residual stress distribution adjusted for equilibrium.

3.3 Discussion of Results

The maximum tensile residual stress measured is 69.8 ksi and is observed at the upper left weld and the maximum compressive residual stress is - 22.4 ksi at about 2 inches from the lower left weld.

Even though the material is ASTM A36 steel, with

a minimum specified yield value of 36 ksi, such high residual stresses are possible at the weld because the deposited weld material has a much higher yield stress than the parent material. To verify this, tension coupon tests were made. The size and location of the small specimens is shown in Fig. 19. Table 2 shows the results of the tension tests. It can be observed that the maximum yield stress of the tension coupons containing the weld is about 65 ksi. The yield stress of the material at the location where the residual stress measurement was taken has apparently a somewhat higher value.

From Fig. 17 it can be observed that the residual stress distribution is not symmetrical. To illustrate the formation of the residual stresses in the box-shape, consider the residual stress distribution of one of the component plates at different stages of the manufacturing procedure. Figure 20 presents results of residual stress measurements of a plate 24" x 2".[9]

Cooling after rolling leaves compressive residual stresses at the edges and tensile residual stresses in the

middle portion. The flame-cutting of the edges changes the distribution to tension at the edges and compression at the middle. The residual stresses are symmetrical because both edges are flame cut simultaneously. To form the shape, weld material is deposited at the edges. The tensile stresses at the edges are raised to a value near or equal to the yield stress of the deposited weld material. To maintain internal equilibrium the compressive residual stresses will also become bigger. The distribution is no longer symmetrical. This is due to the fact that the weld material is not deposited simultaneously at both edges. In the case of the 24 □ 774 shape a large number of passes was required to complete the welds and the welding sequence was rather complicated. Thus, the welding procedure will have the most significant effect on the formation of residual stress, especially the sequence of welding, since it will be responsible for the unsymmetry of the residual stress distribution.

Figure 21 shows a schematic diagram of the welding sequence as is was recorded at the fabrication of the 24 □ 774. A total of 39 passes was used for the four 7/8" groove welds.

By comparing the diagram in Fig. 21 with the residual stress distribution the following observations can be made:

1. The region at weld #1, which was completed last exhibits the highest value of tensile residual stress.

2. The value of tensile residual stress at weld #4, which was completed first has, compared with the other welds, the lowest value of tensile residual stress.

3. The values of tensile residual stress at welds #1 and #3, which required only nine passes show higher values of residual stress than the welds #2 and #4, which required 11 and 10 passes.

The following conclusions can be stated:

1. The welding process has a major influence on the residual stress distribution of a box-shape. The welding introduces high tensile residual stresses at the weld which have

values near to the yield strength of the deposited weld material. The material at the weld is heat-affected and in general exhibits a yield strength which is much higher than that of the parent material. To maintain internal equilibrium the tensile stresses are balanced by compressive stresses at the middle of the component plates.

2. The unsymmetry of the residual stress distribution is due to the fact that the welds were not welded simultaneously but were completed following a certain sequence. How the residual stress distribution actually is related to the welding sequence should be subject to further research.

3.4 Comparison with Smaller Shapes

The results of measurements of residual stresses in the heavy box-shape were compared with those of earlier studies on smaller box shapes,[10] to evaluate the main differences between heavy and small to medium size shapes.

The residual stress distribution in a 10" x 10" box-shape with $\frac{1}{2}$" thick component plates is shown in Fig. 22.

The following conclusions can be made from this limited comparison:

1. Tensile stresses in the weld region are of higher magnitude in heavy shapes, probably because the restraint is larger.

2. Compressive residual stresses in medium-size shapes are of higher magnitude and almost constant at the center portion of the component plates, whereas the compressive stresses in heavy shapes are smaller in magnitude and decrease towards the center of the plate. This fact was found to be true also for other heavy shapes.[3]

4. EVALUATION OF COLUMN STRENGTH

4.1 Theory and Assumptions

For the evaluation of column strength a computer program was developed based on a theoretical approach described in detail in Ref. 11. The theoretical approach is essentially the same as that used in earlier studies.[4,15]

The following assumptions were made:

1. Each fiber of the column has an idealized linear elastic-plastic stress strain behavior.

2. The initial as well as the final deflected shape is described by a half-sine wave.

3. Residual stresses are uniform through the thickness and constant along the column.

4. Sections originally plane, remain plane for the range of deflections considered.

5. The yield stress σ_y can vary across the column but is assumed to be constant through the thickness of the component plates.

6. The strains and stresses in the cross-section at the column mid-height are considered only.

The main principle of the approach described here is to find a thrust P for any deflection δ at the column mid-height, such that the external and internal forces and moments are in equilibrium.

The two equilibrium equations are:

$$P = P_{int} \tag{1a}$$

$$P\delta = M_{int} \tag{1b}$$

combining (1a) and (1b) yields:

$$P_{int} = \frac{M_{int}}{\delta} \tag{2}$$

Referring to Fig. 23, δ consists of the initial out-of-straightness, the deflection of the column under load, and the eccentricity of the applied thrust:

$\delta = v_o + v_M + e_x$ for y-axis bending

$\delta = u_o + u_M + e_y$ for x-axis bending

A numerical iteration procedure is employed to solve Eq. 2. The shape is divided into a number of finite area elements as shown in Fig. 24. The residual stress and the yield

stress is assumed to be constant inside every element, and along its length.

The total stress in every element due to the applied load can be written as:

$$\frac{\sigma_n}{\sigma_y} = \frac{\epsilon_n}{\epsilon_y} = \bar{\epsilon}_r + \bar{\epsilon}_A + \phi\, x_n/\epsilon_y \quad \text{if} \quad |\sigma_n| \leq \sigma_{yn} \tag{3a}$$

or

$$\frac{\sigma_n}{\sigma_y} = \frac{\sigma_{yn}}{\sigma_y} \quad \text{if} \quad \sigma_n > \sigma_{yn} \quad \text{(YIELDING IN TENSION)} \tag{3b}$$

$$\frac{\sigma_n}{\sigma_y} = \frac{\sigma_{yn}}{\sigma_y} \quad \text{if} \quad \sigma_n < \sigma_{yn} \quad \text{(YIELDING IN COMPRESSION)} \tag{3c}$$

where:

σ_n, ϵ_n = stress and strains in the element

$\bar{\epsilon}_r$ = ratio (residual strain)/(global yield strain)

$\bar{\epsilon}_A$ = ratio (axial strain)/(global yield strain)

ϕ = curvature due to v_M

ϵ_y, σ_y = global strain at yield and global yield stress

σ_{yn} = yield stress of the element

x_n = distance of the element from the y-axis.

For a certain value of mid-height deflection, the only unknown in the above equations is the axial strain since the curvature ϕ can be obtained by assuming the deflected shape to be a sine wave:

$$\phi = \frac{\pi^2}{L^2} \cdot v_M \tag{4}$$

where v_M is the deflection at mid-height due to the applied thrust.

By assuming an initial value of $\bar{\epsilon}_A$ the iteration procedure can be started.

The ratios:

$$\frac{P_{int}}{P_y} = \frac{1}{A} \sum_{n=1}^{N} \frac{\sigma_n}{\sigma_y} A_n \tag{5a}$$

and

$$\frac{M_{int}}{P_y} = \frac{1}{A} \sum_{n=1}^{N} \frac{\sigma_n}{\sigma_y} x_n A_n \tag{5b}$$

where

P_{int} = internal force in column mid-height

M_{int} = internal moment in column mid-height

A_n = area of element n

A = area of cross section

$P_y = A\,\sigma_y$ yield load of the cross section

can now be computed.

Next, the equilibrium equation (Eq. 2) is checked:

$$\frac{\Delta P}{P_y} = \frac{P_{int}}{P_y} - \frac{M_{int}}{P_y\,\delta} \leq \Delta_{min} \qquad (6)$$

If $\frac{\Delta P}{P_y}$ exceeds the specified tolerance Δ_{min}, the value of $\bar{\epsilon}_A$ is changed and a new improved value of $\frac{\Delta P}{P_y}$ is computed. The iteration process is continued until $\frac{\Delta P}{P_y} \leq \Delta_{min}$. The value of Δ_{min} used in the program described in this report is 0.002. This means that the iteration is stopped when ΔP is 0.2% of the yield load of the cross-section. The iteration procedure described above is carried out for different values of v_M. For every mid-height deflection the corresponding thrust which satisfies equilibrium is found and a load-deflection curve is obtained. The maximum value of P is the maximum load the column can carry.

Every value of L/r leads to a corresponding value for P_{max} and the column curve can be obtained. Before the computation is started the residual stress distribution is checked for equilibrium and, if necessary, adjusted to ensure equilibrium.

The average central processor time required for computing one column curve of the 24 □ 774 shape with intervals of L/r equal to 10 is about 10-20 seconds on a CDC 6400 computer, and costs about $1.50.[1]

Elastic Unloading

In the theoretical approach described above, it has been assumed that every element will follow the idealized elastic-plastic stress strain curve in the loading as well as in the unloading process. However, it is known that the unloading will be elastic and therefore, will follow a different path. To study the importance of this fact on the column strength the program was modified to include elastic unloading. The additional equation for the element stress can be derived from Fig. 25 for an element unloading elastically in compression:

$$\frac{\sigma_n}{\sigma_y} = \frac{\epsilon_n}{\epsilon_y} - \frac{\epsilon_n^*}{\epsilon_y} + \frac{\sigma_{yn}}{\sigma_y} \qquad (7)$$

if $\frac{\epsilon_n}{\epsilon_y} < \frac{\epsilon_n^*}{\epsilon_y}$ and $\frac{\epsilon_n^*}{\epsilon_y} > \frac{\epsilon_{yn}}{\epsilon_y}$

[1] Based on current prices at the Lehigh University Computing Center (1970).

where ϵ_n^* is the value of the element strain at the onset of elastic unloading.

Comparison was made between the values of maximum strength computed with and without elastic unloading. For the values of slenderness and out-of-straightness considered in the next chapters, no significant difference in the maximum strength was found. Even though it was observed that unloading will take place, the effect on the maximum strength will not be very great since fibers will start to unload near or after the maximum load is reached. The elastic unloading will have more effect on the unloading behavior of the column, that is, after the maximum load has been reached.

4.2 Influencing Factors

The maximum load a pinned end column can carry can be defined as a function of a number of variables:

$$P_{max} = P_{max} (\sigma_y, \sigma_r, e_o, v_o, G, A, L/r)$$

where the variables in the parentheses are defined as:

1. Yield stress σ_y

2. Residual stress σ_r
3. Eccentricity of the applied load e_o
4. Initial deflection of the column v_o
5. Geometry of the cross section G
6. Area of the cross section A
7. Young's Modulus E
8. Slenderness of the column L/r

Each of these variables can again be a function of the other variables. For example

$$\sigma_r = \sigma_r \ (G, A)$$

since the residual stress distribution is different for different geometries and sizes. For one particular column these variables are defined and the maximum strength of the column can be computed. However the maximum strength of one particular column is not relevant since we are dealing in practice with a variety of columns. One possible approach is to treat the above mentioned variables as random variables.[12] An extensive investigation is currently underway at Lehigh University to predict the maximum strength of columns based on probabilistic concepts.

The scope of the study presented next is not to predict the maximum strength but to investigate the importance of some of the variables. By choosing two extreme values of some variables and evaluating the column strength with these values, their influence is shown.

The following factors are considered:

1. Initial deflection v_o
2. Residual stress σ_r
3. Slenderness L/r
4. Geometry G and Area A

Except for the slenderness ratio, all the factors were considered separately, that is one factor was varied while the other factors were considered to be constant.

4.3 Results

Influence of Initial Out-of-Straightness

Two column curves for the shape 24 □ 774 were computed with two extreme values, to show the influence of the initial out-of-straightness. A column having the

maximum allowable out-of-straightness[13] was compared with an almost perfectly straight one. The curves for v_o = L/1000 and v_o = L/10000 are shown in Fig. 26. The residual stress distribution was assumed to be symmetrical and based on the results obtained in the previous chapters (see Fig. 27). The distribution of the yield stress across the shape is assumed, based on the tension coupon test results (see Fig. 28). Bending about the x-axis was considered only.

Influence of Residual Stress

Again, two extreme cases were chosen to study the influence of residual stress on the column strength of the heavy box-shape. A column having no residual stress is compared with one containing residual stress as shown in Fig. 27. Figure 29 shows these two curves for v_o = L/1000.

To evaluate the influence of an unsymmetric residual stress distribution the maximum strength curves for the 24 □ 774 shape were computed with the unsymmetrical residual stress distribution obtained from the residual stress measurements (see Fig. 30). The result for v_o = L/1000 and v_o = L/10000 is plotted in Fig. 31.

Two cases are considered:

Case 1: The higher compressive residual stress is at the concave side of the column.

Case 2: The lower compressive residual stress is at the concave side of the column.

It is assumed that the column will buckle in the direction of the initial deflection.

4.4 Discussion of Results

The initial out-of-straightness and the residual stress have a significant influence on the column strength. The fact that the column will not be perfectly straight can influence the maximum strength significantly; the reduction can be as much as 12%. The influence is almost constant over the region of slenderness ratios considered if v_o is expressed in terms of the length of the column. The presence of symmetrical residual stress can decrease the maximum strength as much as 10% from the condition without residual stresses. The influence will become smaller for slender columns.

The fact that the residual stress distribution in the 24 □ 774 shape is not symmetrical will effect the column strength of medium length columns ($L/r < 90$), having a small initial out-of-straightness. The column strength depends in this case on the location of the higher compressive residual stress. The column curves in Fig. 31 begin to diverge for slenderness ratios below 100, the lower curves representing the column which has the higher compressive residual stress at the concave side, that is the side where higher compressive stresses are applied due to bending. The difference between these two curves can be as much as 4% ($v_o = L/1000$) and 12% ($v_o = L/10000$).

For the column curves in Fig. 27 it has been assumed that the buckling will occur in the direction of the initial out-of-straightness. It has been observed however in tests of initially very straight columns that a column can first start to deflect in the direction of the initial deflection, but, after a certain load is reached, can deflect in the opposite way. This phenomenon of deflection reversal has been observed on rolled columns

which had significant unsymmetric residual stresses due to cold-straightening.[14]

Almost 14 years ago, Fujita[15] made the unsymmetrical residual stress alone responsible for the occurrence of deflection reversal. However, his theoretical approach is very simple and does not represent the actual case. Apparently the variation of residual stress along the length and the initial shape of the column also has some influence.

4.5 Comparison With a Smaller Shape

To evaluate the differences in maximum strength between heavy box-shapes and smaller shapes, column curves for both shapes were computed.

Figure 32 shows two column curves: one was computed for the heavy box-shape 24 □ 774, the other for a small- to medium-size box-shape 10 □ 61. The residual stress distribution for the smaller shape was obtained from Ref. 10. The initial out-of-straightness for both columns was assumed to be L/1000.

Since the maximum load is non-dimensionalized by the yield load P_y in the plot and in both cases the material used was ASTM A36, these two curves can be compared.

For large slenderness ratios ($L/r > 100$), the heavy shape can be about 20% stronger than the medium-size one, if compared on a non-dimensionalized basis. As the slenderness decreases, the difference becomes smaller and for shorter columns ($L/r < 60$) the medium-size shape tends to be about 3% stronger. Comparison with column test results for the 10 □ 61 box-shape (Ref. 16) show a good agreement with the theoretical prediction.

5. SUMMARY AND CONCLUSIONS

This report presents the results of an investigation on a heavy welded box shape 24 □ 774. The study was both experimental and theoretical.

The residual stress distribution of the heavy box-shape was measured and the variation of yield stress was determined using tension coupon tests. A computer program was developed to study the influence of residual stresses on the maximum strength of a column. Comparison was made with a small to medium size shape 10 □ 61. Even though this investigation dealt with only one heavy and one medium-size box-shape, some characteristic tendencies were observed and explained, and the main differences between heavy and medium-size shapes were evaluated.

Based on the shapes studied, the following conclusions can be stated.

1. Tensile residual stresses in the region of the welds tend to be of higher magnitude in

heavy box-shapes than in small to medium-size box-shapes. This is probably due to the fact that the restraint in heavy shapes is bigger.

2. The yield stress of the material near the weld can have a value which is nearly twice that of the parent material, reflecting the weld metal and the heat-treatment.

3. Compressive residual stresses at the middle of the component plates tend to be lower for the heavy box-shapes as compared to the much smaller size box-shapes.

4. The welding procedure, especially the sequence of welding, has the most significant influence on the formation of residual stress. The sequence of welding causes the residual stress distribution to be unsymmetrical.

5. The unsymmetry of the residual stress distribution becomes significant for medium-length columns ($L/r < 90$) having a small initial out-of-straightness.

6. From a comparison between the heavy shapes 24 □ 774 and the small- to medium-size shape 10 □ 61 it has been observed that slender heavy columns ($L/r > 100$) can exhibit a value of maximum strength which can be as much as 20% higher than that of the slender medium-size column. As the slenderness decreases, the difference becomes smaller and for $L/r < 70$ it reverses (that is, the medium-size column tends to be slightly stronger than the heavy one).

The study presented here is limited and more research on heavy shapes has to be conducted in the future. However, the attempt has been made to point out the factors which have significant influence both on the formation of residual stress and on the strength of heavy box-columns. It has been shown that the welding procedure and sequence has a significant influence on the formation of residual stress and that the resulting dissymmetry of residual stresses can have some effect on column strength.

For the heavy box-shape, about 2000 measurements had to be taken to obtain the residual stress distribution. The time required to section the specimen was considerable, mainly because some shopwork had to be done elsewhere, since the facilities were not available at Fritz Engineering Laboratory to handle such large shapes.

Since the experimental investigation is very costly and time-consuming, more emphasis should be given in the future to the theoretical prediction of residual stress. A computer program should be developed to predict residual stresses in any heavy shape, including the effect of the welding sequence; this would build on the earlier work conducted at Lehigh University a decade ago. Thus, test specimens would be used only to confirm the theory.

6. NOMENCLATURE

A	Area of the cross section
A_n	Area of the finite area element
B, D, T	Dimensions of the cross section
E	Young's Modulus
e_x, e_y	Eccentricity of the applied load
L	Length of column
M_{int}	Internal moment
n	Number of finite area element
P	External applied thrust
P_{int}	Internal thrust
r	Radius of gyration
u_o, v_o	Initial deflection at column mid-height
u_M, v_M	Deflection due to applied load at column mid-height
x_n, y_n	Coordinates of finite area elements
δ	Total deflection at column mid-height
ϵ_n	Total element strain
$\bar{\epsilon}_R$	Non-dimensionalized residual element strain
$\bar{\epsilon}_A$	Non-dimensionalized axial element strain

ϵ_y	Global strain at yield
ΔP	Out-of-equilibrium force
Δ_{min}	Tolerance limit for the out-of-equilibrium force
σ_n	Total element stress
σ_y	Global yield stress
σ_{yn}	Yield stress of the element
ϕ	Curvature due to external load.

7. TABLES AND FIGURES

TABLE 1

CHEMICAL AND MECHANICAL PROPERTIES OF THE HEAT*

Yield Point (ksi)	Tensile Strength (ksi)	C %	Mn %	P %	S %	Si %
37.0	65.5	.18	1.00	.012	.020	.25

*As given in the mill test report.

TABLE 2

TENSION SPECIMEN TEST RESULTS, 24 □ 774

(ASTM A36 Steel, E7018 Electrode)

Tension Specimen No.	Static Yield Stress (ksi) €=.005	Dynamic Yield Stress (ksi)	Ultimate Stress (ksi)	Reduction of Area (%)	Elong. in Gage Length** (%)
1	65.5	67.9	82.5	58.5	26.5
2	47.5	49.6	73.4	61.0	30.0
3	—*	—*	67.1	59.5	35.0
4	62.9	65.2	81.5	57.8	26.5
5	45.0	46.8	69.7	61.3	24.5
6	—*	—*	60.5	64.5	42.0
7	64.0	66.5	80.7	57.0	30.0
8	45.6	47.6	72.1	59.0	34.0
9	—*	-*	66.2	48.7	35.1
10	45.0	47.0	71.0	59.5	31.5
11	63.0	65.1	81.3	56.9	22.5
12	29.2	30.6	62.0	62.4	42.0

*No yield-point observed.
**2" gage length.

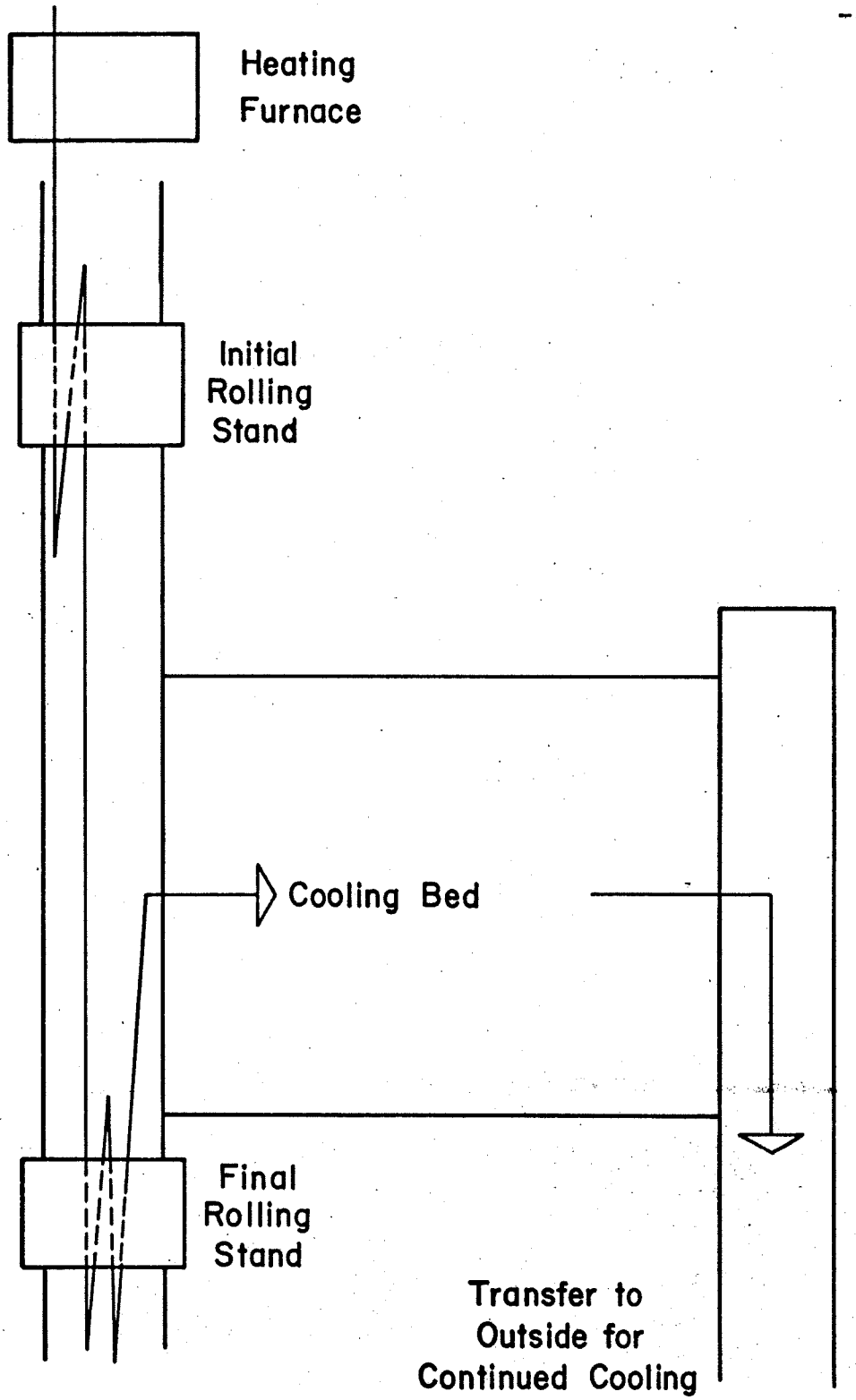

Fig. 3 Rolling Process (Schematic Path)

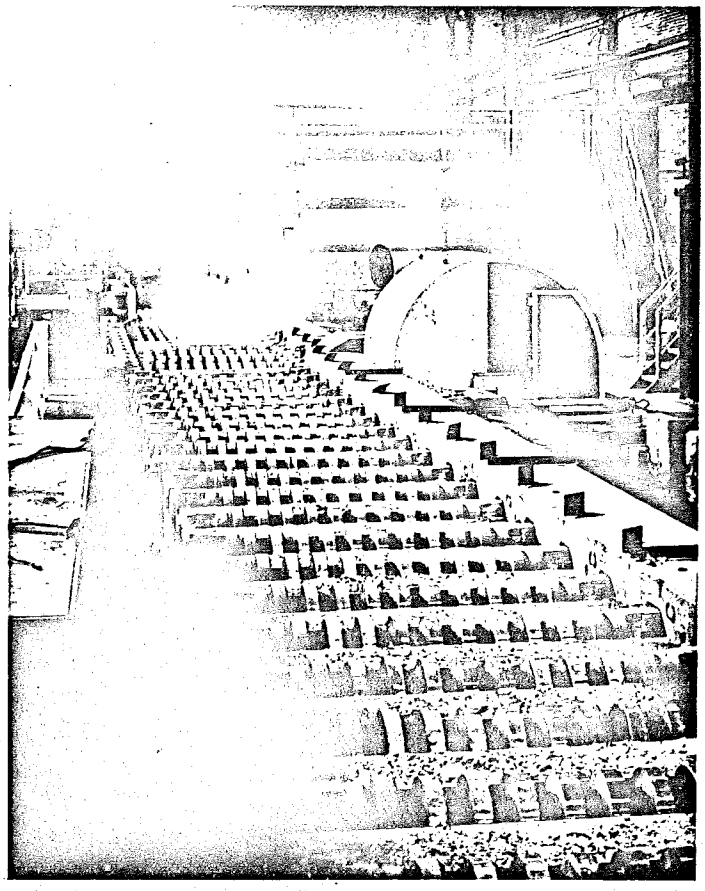

Fig. 4 Rolling Process

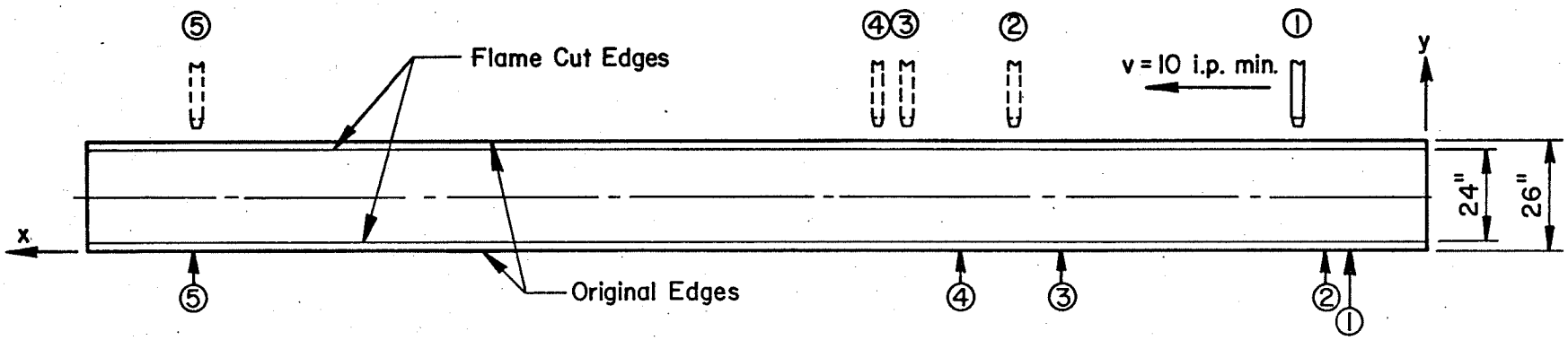

Location Number	Time (Min.)	X Cordinate of Nozzle (in.)	Distance Between Section of Meas. and Nozzle (in.)
1	4:00	40	13
2	13:30	135	100
3	17:00	170	50
4	18:00	180	25
5	40:00	400	2

Symbols	
	Location of the Nozzle
	Location of Measurements

Fig. 6 Relative Position of Nozzle and Temperature Measurement

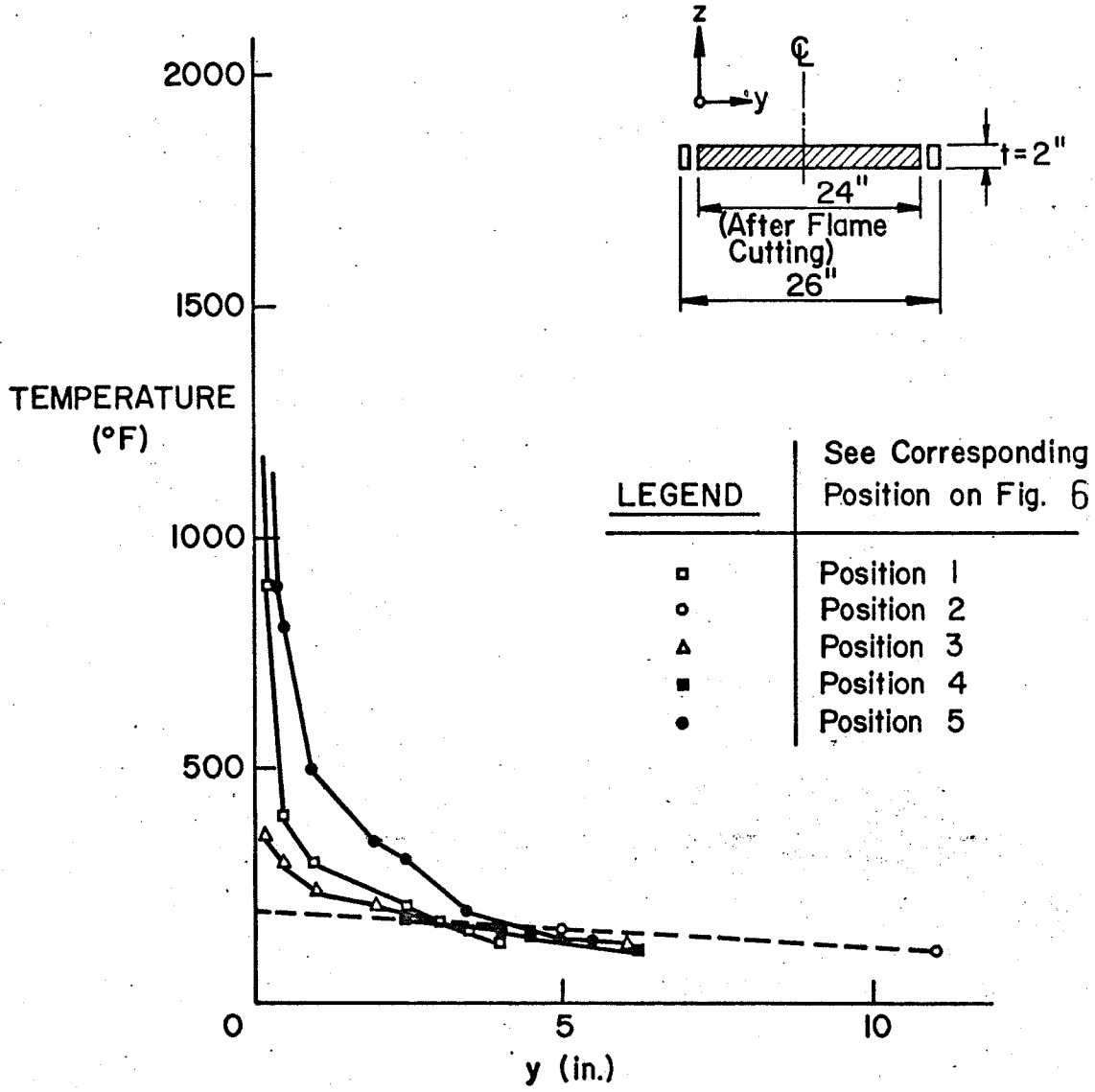

Fig. 7 Temperature Distribution Due to Flame-Cutting

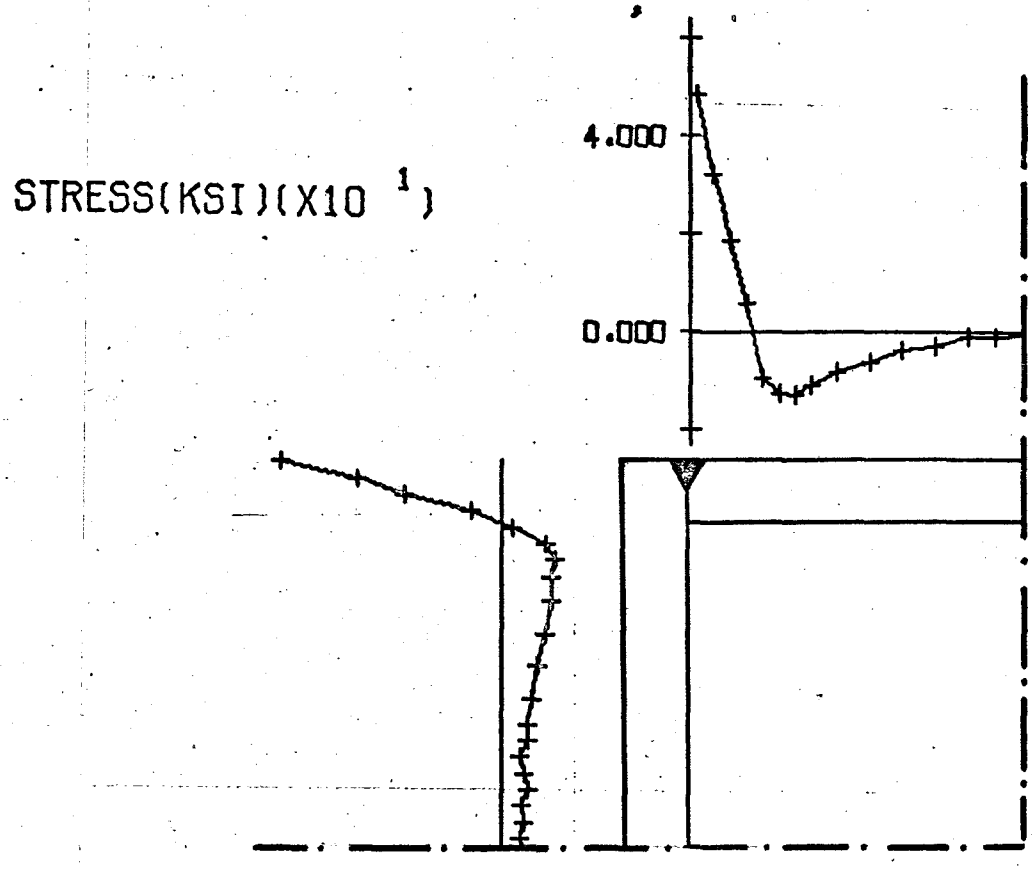

Fig. 27 Average Residual Stress Symmetric With Respect to x- and y-axes

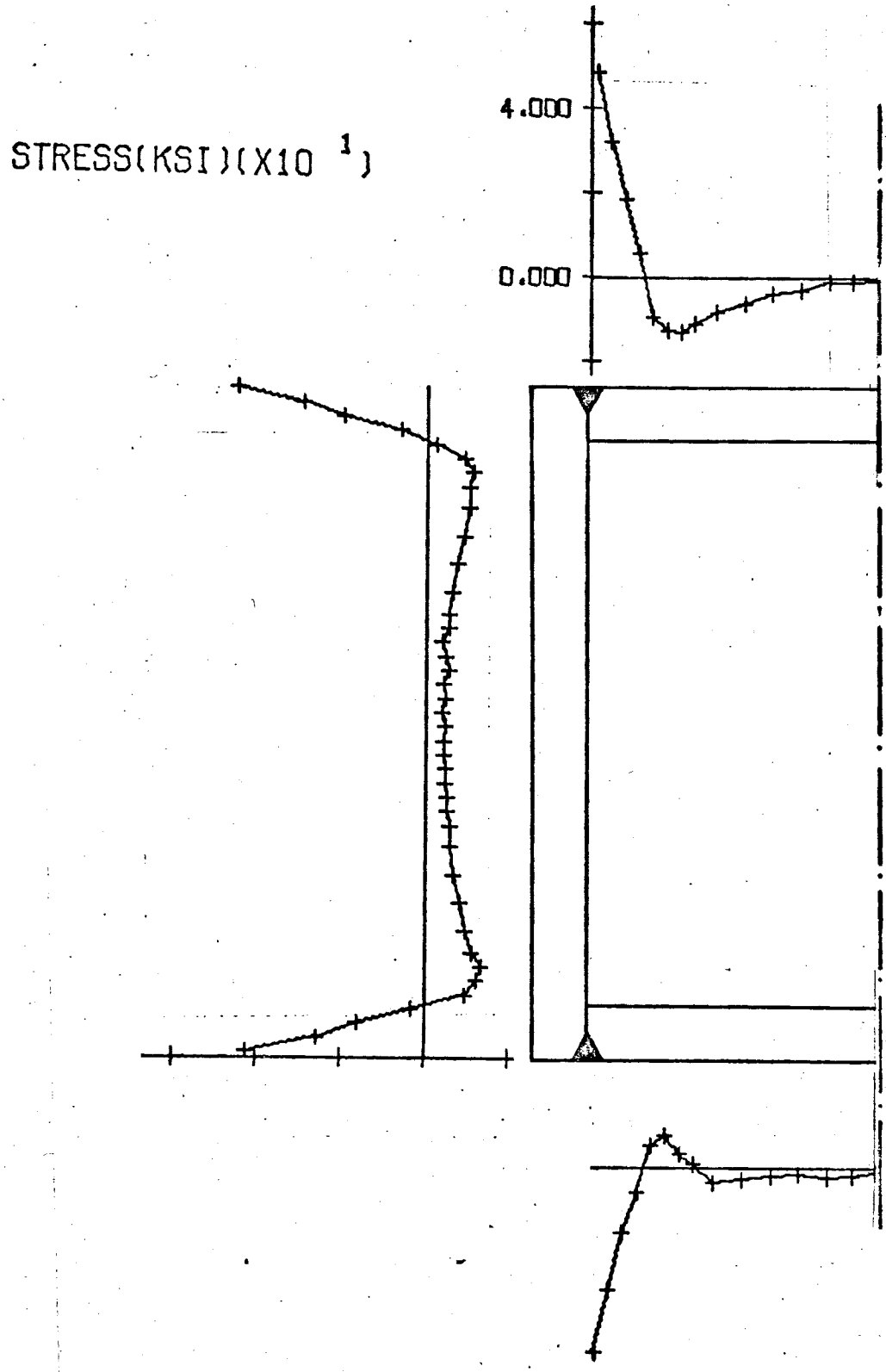

Fig. 30 Average Residual Stress Unsymmetric With Respect to y-axis but Symmetric With Respect to x-axis

8. APPENDIX

Flowchart and Listing of the Computer Program

SIMPLIFIED FLOWCHART FOR PROGRAM "MAXLOAD"

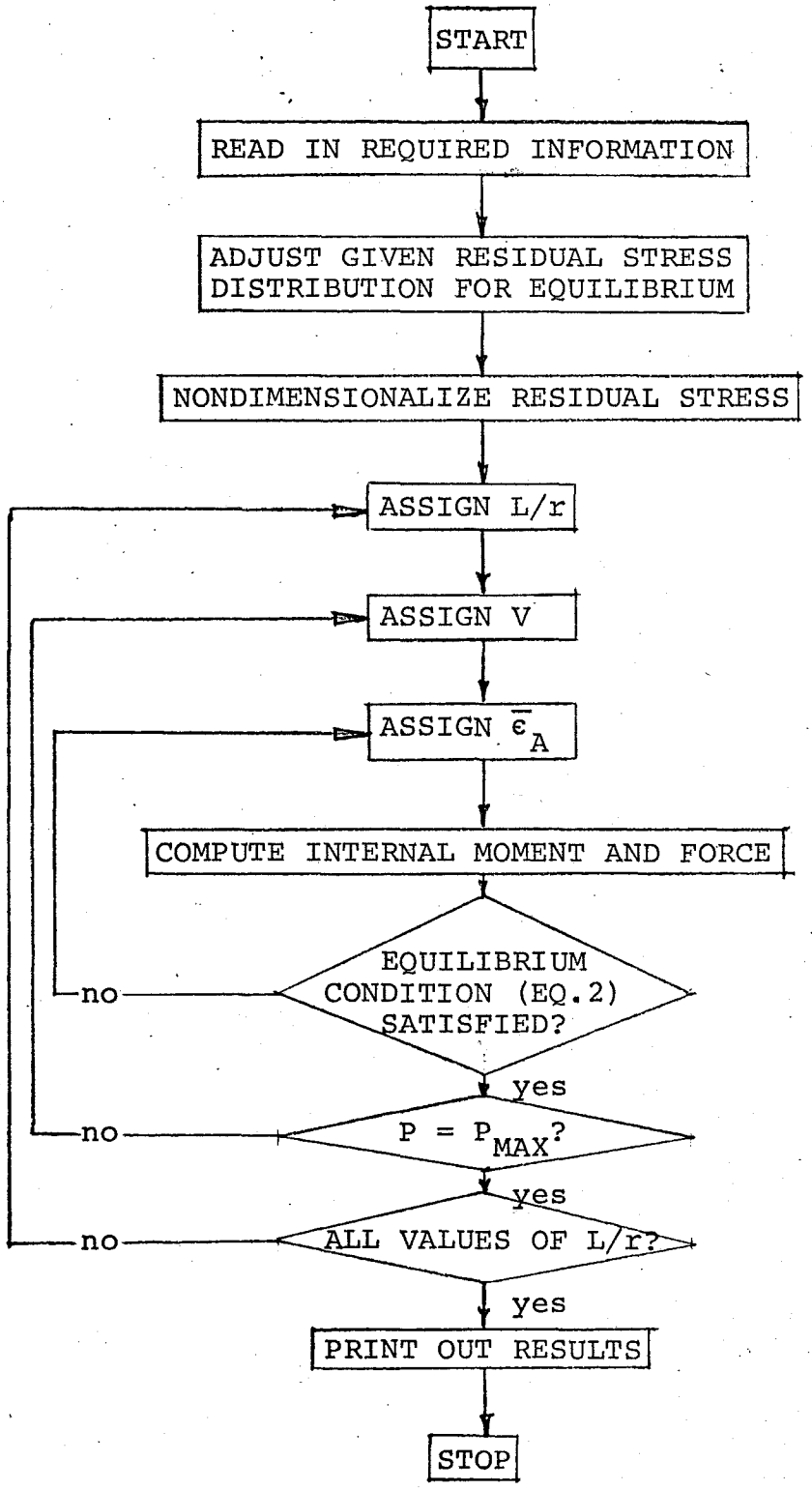

```
      PROGRAM MAXLD(INPUT,TAPE1=INPUT,OUTPUT,TAPE2=OUTPUT)
C*****************************************************************
C
C  COMPUTATION OF THE MAXIMUM STRENGTH OF BOX COLUMNS
C
C  LEHIGH UNIVERSITY, FALL 1970      PROGRAMMER.. G. BEER
C  TESTED AT A CONTROL DATA CORPORATION 6400 COMPUTER
C  WRITTEN IN FORTRAN IV
C  COMPILED ON SCOPE 3.2
C
C     ASSUMPTIONS.
C
C  1. EVERY FIBER HAS AN IDIALISED LINEAR ELASTIC PLASIC STRESS-STRAIN
C     RELATION SHIP
C  2. THE INITIAL AND FINAL DEFLECTED SHAPE IS DESCRIBED BY A HALF SINE
C     WAVE
C  3. YIELDED FIBERS UNLOAD ELASTICALLY
C  4. RESIDUAL STRESSES ARE UNIFORM TROUGH THE THICKNESS AND CONSTANT
C     ALONG THE LENGTH
C  5. PLAIN SECTIONS REMAIN PLAIN
C  6. CROSSECTION AT MIDHEIGHT IS CONSIDERED ONLY
C
C*****************************************************************
      DIMENSION RESTF1(50), RESTW1(50), RESTF2(50), RESTW2(50), Y1(50),
     1X1(50), F1ST(50), F1S(50), F2ST(50), F2S(50), W1ST(50), W1S(50), W
     22ST(50), W2S(50), NCO(50), NTE(50)
      DIMENSION IF1(50), IF2(50), SYF(50), SYW(50), IW1(50), IW2(50)
      COMMON /1/ RSTF1(50),RSTF2(50),RSTW1(50),RSTW2(50),NW,NF,NAME,OUT
      COMMON /2/ SF,MOMENT,BASTR,PHI,YSTR,SWITCH
      COMMON /3/ T
      COMMON /4/ DX(50),DY(50),X(50),Y(50),XI,YI,XA,YA,AREA,D,B
      COMMON /5/ XAA(50),YAA(50),XAAM(50),YAAM(50)
      COMMON /6/ NYT,NYC,NEL
      REAL L,MOMLD,MOMENT,LOR
      INTEGER OUT,SWA,SWB
      LOGICAL NEL
      IN=1
      OUT=2
C     READ REQUIRED INPUT
      READ (IN,46) NAME
      READ (IN,42) NCYCLE
      READ (IN,42) NF,NW
      READ (IN,45) B,D,T,XA,YA
      READ (IN,45) (DX(J),J=1,NF)
      READ (IN,45) (DY(J),J=1,NW)
      READ (IN,45) (X(J),J=1,NF)
      READ (IN,45) (Y(J),J=1,NW)
      READ (IN,42) IMAX
      READ (IN,45) YS
      READ (IN,47) (SYF(J),J=1,NF)
      READ (IN,47) (SYW(J),J=1,NW)
      WRITE (OUT,54) NAME
      AREA=2.*B*T+2.*D*T
      WRITE (OUT,48) B,D,T,AREA
      WRITE (OUT,53)
      WRITE (OUT,51) (SYF(J),J=1,NF)
      WRITE (OUT,52) (SYW(J),J=1,NW)
```

```
      READ (IN,45) (RSTF1(J),J=1,NF)
      READ (IN,45) (RSTW1(J),J=1,NW)
      READ (IN,45) (RSTF2(J),J=1,NF)
      READ (IN,45) (RSTW2(J),J=1,NW)
C  SPECIFY CONSTANTS
      ISW=0
      PI=3.1416
      C=T/AREA
      YSTR=YS/29600.
      PY=YS*AREA
C     ADJUST RESIDUAL STRESS-DISTRIBUTION FOR EQUILIBRIUM
      CALL ADJUST
      SWITCH=1.0
C
C  OPT=X , ISYM=1    X-AXIS BENDING
C  OPT=Y , ISYM=0    Y-AXIS BENDING
C
      READ (IN,44) OPT,ISYM
      IF (ISYM.EQ.1) R=XI
      IF (ISYM.EQ.0) R=YI
      R=SQRT(R/AREA)
C     NONDIMENSIONALIZE RESIDUAL STRESS
      DO 1 J=1,NF
      RESTF2(J)=-RSTF2(J)/YS
    1 RESTF1(J)=-RSTF1(J)/YS
      DO 2 J=1,NW
      RESTW2(J)=-RSTW2(J)/YS
    2 RESTW1(J)=-RSTW1(J)/YS
    3 READ (IN,45) EOL
C
C  NEL=.TRUE.    ELASTIC UNLOADING OF FIBERS CONSIDERED
C  NEL=.FALSE.    ELASTIC UNLOADING OF FIBERS NOT CONSIDERED
C
    4 READ (IN,43) NEL
    5 ISW=ISW+1
      READ (IN,45) LOR
      IF (LOR.GE.200.) GO TO 3
      IF (LOR.EQ.0.) GO TO 4
      IF (LOR.LT.0.) GO TO 41
      READ (IN,49) VINCR,BAINCR,ASTART,VSTART
      L=LOR*R
      V0=EOL*L
      WRITE (OUT,55) OPT,LOR,L,YS,V0
      WRITE (OUT,50) NEL
C
C     INITIALISE VALUES
C
      NYC=0
      NYT=0
      BASTR=ASTART
      V=VSTART
      AXLOAD=0.
      DEFL=V0
      NUM=0
      DO 6 J=1,NF
      IF1(J)=0
      IF2(J)=0
      F1ST(J)=0.
```

```
    6 F2ST(J)=0.
      DO 7 J=1,NW
      IW1(J)=0
      IW2(J)=0
      W1ST(J)=0.
    7 W2ST(J)=0.
    8 NUM=NUM+1
C
C     STORE COMPUTED VALUES INTO ARRAY
C
      NCO(NUM)=NYC
      NTE(NUM)=NYT
      Y1(NUM)=AXLOAD
      X1(NUM)=V
      IF (NUM.EQ.IMAX) GO TO 38
      IF (NUM.EQ.1) GO TO 9
      IF (Y1(NUM).LE.Y1(NUM-1)) GO TO 38
    9 BASTR=BASTR+BAINCR
      V=V+VINCR
      DO 11 J=1,NF
      IF (IF1(J).EQ.1) GO TO 10
      F1S(J)=F1ST(J)
   10 IF (IF2(J).EQ.1) GO TO 11
      F2S(J)=F2ST(J)
   11 CONTINUE
      DO 13 J=1,NW
      IF (IW1(J).EQ.1) GO TO 12
      W1S(J)=W1ST(J)
   12 IF (IW2(J).EQ.1) GO TO 13
      W2S(J)=W2ST(J)
   13 CONTINUE
C  DEL ...FIRST ITERATION STEP
      DEL=.05
      PHI=PI*PI*V/(L*L)
      DEFL=V0+V
      SWA=0
      IC=0
      ITER=0
      M=0
      MU=0
C  START ITERATION TO OBTAIN P/PY FOR A SPECIFIC VALUE OF V
   14 ITER=ITER+1
      IF (ITER.GE.NCYCLE) GO TO 40
C  INTEGRATE ACROSS SHAPE TO OBTAIN INTERNAL MOMENTS AND FORCE
C  BENDING ABOUT Y-AXIS
      IF (ISYM.EQ.1) GO TO 15
      CALL SUMSTR (RESTF1,X,SYF,DX,NF,F1ST,F1S,IF1)
      CALL SUMSTE (RESTW1,XAA,SYW,DY,NW,W1ST,W1S,IW1)
      CALL SUMSTE (RESTF2,X,SYF,DX,NF,F2ST,F2S,IF2)
      CALL SUMSTE (RESTW2,XAAM,SYW,DY,NW,W2ST,W2S,IW2)
      GO TO 16
C  BENDING ABOUT X-AXIS
   15 CALL SUMSTR (RESTW1,Y,SYW,DY,NW,W1ST,W1S,IW1)
      CALL SUMSTE (RESTF1,YAA,SYF,DX,NF,F1ST,F1S,IF1)
      CALL SUMSTE (RESTW2,Y,SYW,DY,NW,W2ST,W2S,IW2)
      CALL SUMSTE (RESTF2,YAAM,SYF,DX,NF,F2ST,F2S,IF2)
   16 MOMLD=(MOMENT/DEFL)*C
      AXLOAD=SF*C
```

```
      MOMLD=-MOMLD
C     CHECK EQUILIBRIUM CONDITION
C     IF ACCURACY SUFFICIENT GOTO NEXT VALUE OF V
      DELTA=AXLOAD-MOMLD
      IF (ABS(DELTA).LE..002) GO TO 8
      IF (MOMLD.EQ.0.) GO TO 39
C
C     THE FOLLOWING STATEMENTS CONTROL THE ITERATION PROCEDURE AND
C     CHANGE THE VALUE OF BASTR AT EVERY ITERATION CYCLE SUCH THAT
C     FAST CONVERGENCE IS OBTAINED
C
      IF (SWA) 17,21,17
   17 IF (DELTA) 18,19,19
   18 SWB=-1
      GO TO 20
   19 SWB=1
   20 IF (SWB-SWA) 30,31,30
   21 IF (DELTA) 22,23,23
   22 SWA=-1
      GO TO 24
   23 SWA=1
   24 IF (ABS(DELTA).LE.0.02) GO TO 29
      IF (M) 28,25,28
   25 IF (DELTA) 27,27,26
   26 M=-1
      GO TO 28
   27 M=1
   28 BASTR=BASTR+DEL*M
      GO TO 14
   29 DEL=.002
      IF (M) 28,25,28
   30 IF (IC) 32,34,33
   31 IF (IC) 33,24,32
   32 MU=1
      GO TO 37
   33 MU=-1
      GO TO 37
   34 IF (M) 35,41,36
   35 IC=-2
      GO TO 32
   36 IC=1
      GO TO 33
   37 DEL=DEL/2.
      BASTR=BASTR+MU*DEL
      GO TO 14
C
C     PRINT OUT RESULTS
C
   38 Y1MAX=Y1(NUM-1)
      WRITE (OUT,56) (X1(J),Y1(J),NCO(J),NTE(J),J=1,NUM)
      WRITE (OUT,57) Y1MAX
      Y1MAX=Y1MAX*PY
      WRITE (OUT,58) Y1MAX
      GO TO 5
C
C     PRINT OUT ERROR MESSAGES
C
   39 WRITE (OUT,59)
```

```
   40 WRITE (OUT,60) ITER
      WRITE (OUT,61)
      WRITE (OUT,62)
      WRITE (OUT,63) BASTR,AXLOAD,MOMLD,DELTA
      GO TO 8
   41 CALL EXIT
C
   42 FORMAT (I2,1X,I2)
   43 FORMAT (L1)
   44 FORMAT (A1,I1)
   45 FORMAT (10F8.0)
   46 FORMAT (A10)
   47 FORMAT (20F4.0)
   48 FORMAT (1H0,* DIMENSIONS*//1H ,* B=*F8.3/1H * D=*F8.3/1H * T=*F8.3
     1/1H * AREA=*F8.3/)
   49 FORMAT (4F5.0)
   50 FORMAT (1H0,*   ELASTIC UNLOADING=*L5/)
   51 FORMAT (1H ,*(FLANGE)*8F7.2)
   52 FORMAT (1H ,*(WEB)*F7.2)
   53 FORMAT (1H0,* YIELDSTRESS-DISTRIBUTION(SY/SYG)*//)
   54 FORMAT (1H1,3X,A10)
   55 FORMAT (1H1* COLUMN STRENGTH WITH BENDING ABOUT *A1*-AXIS PERMITTE
     1D*/1H0* L/R=*F8.2* L=*F8.2* YIELDSTRESS=*F8.2* V0=*F8.4)
   56 FORMAT (1H0,*  V=*,F7.4,*  P/PY=*,F7.4,3X,I4* ELEMENTS YIELDED IN
     1COMPR.*I4* IN TENSION*)
   57 FORMAT (1H0,*  PU/PY=*,F10.4)
   58 FORMAT (1H0,*  PU=*,F10.0)
   59 FORMAT (1H0,23H******ERROR ENCOUNTERED)
   60 FORMAT (1H0,36H******CONVERGENCE NOT OBTAINED AFTER,I10,8H  CYCLES
     1)
   61 FORMAT (1H0,22HLAST ITERATION CYCLE../)
   62 FORMAT (1H0,12H   BASTR    ,3X,17HP/PY(AXIAL EQUIL),3X,17HP/PY(MOM
     1ENTEQUIL),3X,10HDIFFERENCE/)
   63 FORMAT (1H ,4(F12.7,6X))
      END
```

```
      SUBROUTINE SUMSTR (RESTR,X,SY,DX,N,STRAIN,STRN,IF)
C*****************************************************************
C
C  THIS SUBROUTINE PERFORMES THE NUMERICAL INTEGRATION OF STRESSES
C  ALONG ONE COMPONENT PLATE OF THE SHAPE TO OBTAIN INTERNAL MOMENT
C  AND FORCE
C  IT ALSO COMPUTES THE NUMBER OF ELEMENTS YIELDED IN COMPRESSION
C  OR IN TENSION
C
C*****************************************************************
      COMMON /2/ SF,MOMENT,BASTR,PHI,YSTR,SWITCH
      COMMON /6/ NYT,NYC,NEL
      DIMENSION RESTR(50), X(50), DX(50), SY(50), STRAIN(50), STRN(50),
     1IF(50)
      REAL MOMENT
      LOGICAL NEL
      SF=0.
      MOMENT=0.
      NYT=0
      NYC=0
      ENTRY SUMSTE
      DO 9 J=1,N
      IF (J) =0
      ELSTRN=RESTR(J)+BASTR-(PHI*X(J))/YSTR
      IF (SWITCH) 1,3,1
    1 STRAIN(J)=ELSTRN
      CHECKS=STRN(J)
      ELYSTR=SY(J)
      IF (.NOT.NEL) GO TO 2
      IF (CHECKS.GT.ELYSTR) GO TO 5
      IF (CHECKS.LT.-ELYSTR) GO TO 4
C   ELEMENT HAS NOT YIELDED AT PREVIOUS LOAD
    2 IF (ELSTRN.LT.-ELYSTR) GO TO 6
      IF (ELSTRN.GT.ELYSTR) GO TO 7
    3 STRESS=ELSTRN
      GO TO 8
C   ELEMENT IS YIELDING FURTHER IN TENSION
    4 IF (ELSTRN.LT.CHECKS) GO TO 6
C   ELEMENT IS UNLOADING ELASTICALLY
      STRESS=ELSTRN-CHECKS-ELYSTR
      IF (J) =1
      GO TO 8
C   ELEMENT IS YIELDING FURTHER IN COMPRESSION
    5 IF (ELSTRN.GE.CHECKS) GO TO 7
C   ELEMENT IS UNLOADING
      STRESS=ELSTRN-CHECKS+ELYSTR
      IF (J) =1
      GO TO 8
    6 STRESS=-ELYSTR
      NYT=NYT+1
      GO TO 8
    7 STRESS=ELYSTR
      NYC=NYC+1
    8 FELE=STRESS*DX(J)
      SF=SF+FELE
      DELMOM=FELE*X(J)
    9 MOMENT=MOMENT+DELMOM
      RETURN
      END
```

```
      SUBROUTINE ADJUST
C*****************************************************************************
C
C  THIS SUBROUTINE COMPUTES THE OUT OF EQUILIBRIUM MOMENTS, FORCE
C  AND STRESS OF THE RESIDUAL STRESS DISTRIBUTION.
C  THE RESIDUAL STRESS DISTRIBUTION IS THEN ADJUSTED FOR EQULIBRIUM.
C
C*****************************************************************************
      COMMON /1/ RSTF1(50),RSTF2(50),RSTW1(50),RSTW2(50),NW,NF,NAME,IOUT
      COMMON /2/ SF,MOMENT,BASTR,PHI,YSTR,SWITCH
      COMMON /3/ T
      COMMON /4/ DX(50),DY(50),X(50),Y(50),XI,YI,XA,YA,AREA,D,BA
      COMMON /5/ XAA(50),YAA(50),XAAM(50),YAAM(50)
      DIMENSION SY1(50), A(50)
      INTEGER C(50)
      REAL MOMENT
      DO 1 J=1,NW
    1 SY1(J)=1.
C  COMPUTE MOMENT OF INERTIA
      CALL MINERT (YI,DX,X,NF,D,XA)
      CALL MINERT (XI,DY,Y,NW,BA,YA)
      WRITE (IOUT,8) XI,YI
      WRITE (IOUT,9)
      CALL OUTPUT
      BASTR=.0
      PHI=.0
      SWITCH=.0
      DO 2 J=1,NW
    2 XAA(J)=XA
      DO 3 J=1,NW
    3 XAAM(J)=-XA
      DO 4 J=1,NF
    4 YAA(J)=YA
      DO 5 J=1,NF
    5 YAAM(J)=-YA
C  MOMENT ABOUT Y-AXIS AND AXIAL FORCE
      CALL SUMSTR (RSTF1,X,SY1,DX,NF,A,A,C)
      CALL SUMSTE (RSTW1,XAA,SY1,DY,NW,A,A,C)
      CALL SUMSTE (RSTF2,X,SY1,DX,NF,A,A,C)
      CALL SUMSTE (RSTW2,XAAM,SY1,DY,NW,A,A,C)
      SUMF=SF*T
      SUMY=MOMENT*T
C  MOMENT ABOUT X-AXIS
C
      CALL SUMSTR (RSTW1,Y,SY1,DY,NW,A,A,C)
      CALL SUMSTE (RSTF1,YAA,SY1,DX,NF,A,A,C)
      CALL SUMSTE (RSTW2,Y,SY1,DY,NW,A,A,C)
      CALL SUMSTE (RSTF2,YAAM,SY1,DX,NF,A,A,C)
      SUMX=MOMENT*T
      WRITE (IOUT,10) SUMF
      SUMS=SUMF/AREA
      WRITE (IOUT,11) SUMS
      WRITE (IOUT,12) SUMY
      WRITE (IOUT,13) SUMX
C  ADJUST FOR EQUILIBRIUM
C
      CALL EQUILI (RSTF1,RSTF2,SUMY,YI,X,NF)
```

```
      DO 6 J=1,NW
      RSTW1(J)=RSTW1(J)-SUMS-SUMY/YI*XA
    6 RSTW2(J)=RSTW2(J)-SUMS+SUMY/YI*XA
      CALL EQUILI (RSTW1,RSTW2,SUMX,XI,Y,NW)
      DO 7 J=1,NF
      RSTF1(J)=RSTF1(J)-SUMS-SUMX/XI*YA
    7 RSTF2(J)=RSTF2(J)-SUMS+SUMX/XI*YA
      WRITE (IOUT,14)
      CALL OUTPUT
      RETURN
C
    8 FORMAT (1H0,* IX=*,F10.3,* IY=*,F10.3,* INCH4*)
    9 FORMAT (1H1,* ACTUAL RESIDUAL STRESS DISTRIBUTION*/1H ,* KSI*/)
   10 FORMAT (1H0,* OUT OF EQUILIBRIUM FORCE=*,F10.5)
   11 FORMAT (1H0,* OUT OF EQUILIBRIUM STRESS=*,F10.5)
   12 FORMAT (1H0,* OUT OF EQUILIBRIUM MOMENT MY=*,F10.5)
   13 FORMAT (1H0,* OUT OF EQUILIBRIUM MOMENT MX=*,F10.5)
   14 FORMAT (1H1,* RESIDUAL STRESS-DISTRIBUTION ADJUSTED FOR EQUILIBRIU
     1M*/1H ,* KSI*/)
      END
```

```
      SUBROUTINE OUTPUT
C*****************************************************************************
C
C  THIS SUBROUTINE IS USED TO PRINT OUT A RESIDUAL STRESS DISTRIBUTION
C  IN A CERTAIN PATTERN
C
C*****************************************************************************
      COMMON /1/ RSTF1(50),RSTF2(50),RSTW1(50),RSTW2(50),NW,NF,NAME,IOUT
      WRITE (IOUT,1) NAME
      NF02=(NF+1)/2
      WRITE (IOUT,2) (RSTF1(J),J=1,NF02)
      WRITE (IOUT,3) (RSTW2(J),J=1,NW)
      WRITE (IOUT,2) (RSTF2(J),J=1,NF02)
      WRITE (IOUT,4)
      WRITE (IOUT,2) (RSTF1(J),J=NF02,NF)
      WRITE (IOUT,5) (RSTW1(J),J=1,NW)
      WRITE (IOUT,2) (RSTF2(J),J=NF02,NF)
      RETURN
C
    1 FORMAT (1H0,A10)
    2 FORMAT (1H0,*(FLANGE)*,18F7.2)
    3 FORMAT (1H ,*(WEB)*,F7.2)
    4 FORMAT (1H1)
    5 FORMAT (1H ,100X,*(WEB)*F7.2)
      END
```

```
      SUBROUTINE MINERT (XI,D,X,N,B,XA)
C*****************************************************************
C
C  THIS SUBROUTINE COMPUTES THE MOMENT OF INERTIA OF THE CROSS SECTI
C
C*****************************************************************
      DIMENSION D(50), X(50)
      COMMON /3/ T
      XI=0.
      DO 1 J=1,N
    1 XI=XI+2.*T*D(J)*X(J)*X(J)
      XI=XI+2.*XA*XA*B*T
      RETURN
      END
```

```
      SUBROUTINE EQUILI (RST1,RST2,SUMM,XI,X,N)
C*****************************************************************
C
C  THIS SUBROUTINE IS USED TO ADJUST THE RESIDUAL STRESS DISTRIBUTIO
C  FOR EQUILIBRIUM
C
C*****************************************************************
      DIMENSION RST1(50), RST2(50), X(50)
      DO 1 J=1,N
      RST1(J)=RST1(J)-SUMM/XI*X(J)
    1 RST2(J)=RST2(J)-SUMM/XI*X(J)
      RETURN
      END
```

9. REFERENCES

1. Huber A. W. and Beedle, L. S.
   RESIDUAL STRESS AND THE COMPRESSIVE STRENGTH OF STEEL, The Welding Journal, Vol. 33, 1954.

2. Beedle, L. S. and Tall, L.
   BASIC COLUMN STRENGTH, Proc. ASCE, No. 2355, Vol. 86, ST7, July 1960.

3. Alpsten, G. A. and Tall, L.
   RESIDUAL STRESSES IN HEAVY WELDED SHAPES, Fritz Engineering Laboratory Report No. 337.12, January 1969.

4. Tall, L.
   THE STRENGTH OF WELDED BUILT-UP COLUMNS, Ph.D. Dissertation, Lehigh University, May 1961.

5. Brozzetti, J., Alpsten, G. A. and Tall, L.
   MANUFACTURE AND FABRICATION OF HEAVY WELDED PLATE AND SHAPE SPECIMENS, Fritz Engineering Laboratory Report No. 337.4, May 1969.

6. CODE FOR WELDING IN BUILDING CONSTRUCTION, American Welding Society, 8th Edition, 1966.

7. Tebedge, N.
   MEASUREMENT OF RESIDUAL STRESS - A STUDY OF METHODS, M.S. Thesis, Lehigh University, 1969.

8. Beer, G. and Tall, L.
   AUTOMATIC PLOTTING OF RESIDUAL STRESS DIAGRAMS, Fritz Engineering Laboratory Report No. 337.26, November 1970.

9. Brozzetti, J. and Tall, L.
   WELDING PARAMETERS AND THEIR EFFECT ON COLUMN STRENGTH, Fritz Engineering Laboratory Report No. 337.21, Feb. 1970.

10. Rao, N. R. N., Estuar, F. R., and Tall, L.
RESIDUAL STRESSES IN WELDED SHAPES, Welding Journal, Vol. 43, July 1964.

11. Beer, G. and Marek, P.
MAXIMUM STRENGTH COMPUTER PROGRAM FOR PINNED-END COLUMNS, Fritz Engineering Laboratory Report No. 337.27 (in preparation).

12. Strating, J.
PROBABILITY THEORY AND BUCKLING CURVES, C.E.A.C.M. Committee 8-1, August 1970.

13. SPECIFICATION FOR THE DESIGN, FABRICATION AND ERRECTION OF STRUCTURAL STEEL FOR BUILDINGS, American Institute of Steel Construction, February 1969.

14. Tebedge, N., Marek, P. and Tall, L.
EUROPEAN COLUMN STUDIES, Fritz Engineering Laboratory Report No. 351.4 (in preparation).

15. Fujita, Y.
BUILT UP COLUMN STRENGTH, Fritz Engineering Laboratory Report No. 249.2, 1956.

16. Estuar, F. R. and Tall, L.
EXPERIMENTAL INVESTIGATION OF WELDED BUILT-UP COLUMNS, Welding Journal, Vol. 42, April 1963.

17. Tall, L.
RESIDUAL STRESSES IN WELDED PLATES - A THEORETICAL STUDY, Welding Journal, Vol. 43, January 1964.